The prompt GRB high energy emission from internal shocks: synchrotron vs inverse Compton component

Zeljka Bosnjak, Frédéric Daigne, and Guillaume Dubus

Citation: AIP Conference Proceedings **1133**, 391 (2009); doi: 10.1063/1.3155927
View online: http://dx.doi.org/10.1063/1.3155927
View Table of Contents: http://scitation.aip.org/content/aip/proceeding/aipcp/1133?ver=pdfcov
Published by the AIP Publishing

The prompt GRB high energy emission from internal shocks: synchrotron vs inverse Compton component

Zeljka Bosnjak[*], Frédéric Daigne[*,†] and Guillaume Dubus[**]

[*]*Institut d'Astrophysique de Paris, UMR 7095, Université Pierre et Marie Curie-Paris 6*
[†]*Institut Universitaire de France*
[**]*Laboratoire d'Astrophysique de Grenoble, UMR 5571 Université Joseph Fourier*

Abstract. We performed a detailed calculation of gamma-ray burst (GRB) prompt emission in the framework of the internal shock scenario, focusing on the high energy (GeV) bands. In order to follow the evolution of the ultrarelativistic inhomogeneous wind, we combined a model for the dynamics of internal shocks with a detailed calculation of the radiative processes occurring in the shocked medium. We present the resulting synthetic GRB light curves and spectra. We show the spectral evolution that can be expected for different sets of microphysics parameters and parameters of the dynamical evolution, and how the relative importance of synchrotron and inverse Compton components is varying during a burst.

Keywords: gamma-rays: bursts; radiation mechanisms: non-thermal
PACS: 98.70.Rz

INTRODUCTION

The observation of high energy (>100 MeV) spectral components in gamma-ray bursts with the *Fermi gamma-ray space telescope* can provide strong constraints on the present models for the GRB prompt emission phase. In expectation of the first observational results, we performed a detailed calculation of the GRB prompt emission in the framework of the internal shock model ([1]). We present our method and several examples of the resulting synthetic GRBs, and discuss the time-dependent spectral properties.

METHOD: DYNAMICS AND RADIATIVE PROCESSES

To study the high energy emission emerging from the evolution of the relativistic wind in the internal shock scenario, we developed the following modelling tools:

- The relativistic outflow during the internal shock phase is modeled as a succession of colliding layers with varying Lorentz factor (see [2]). We determine the physical conditions (Lorentz factor, particle density and energy density) behind each shock wave that occurrs during the wind expansion.
- In the shocked medium, the electrons are accelerated and magnetic field is amplified. The time evolution of the electron distribution is governed by several radiative processes (we accounted for synchrotron radiation, inverse Compton scattering, synchrotron self-absorption and $\gamma\gamma$ annihilation) that are in competition with the adiabatic cooling due to relativistic expansion. The emitted photon spectrum is computed in the comoving frame of the shocked region.
- The overall burst spectrum and time profiles are obtained by adding up the contributions arising from all the internal elementary shocks that occur during the expansion. Each spectrum is transformed to the observer frame accounting for the relativistic effects, the geometry (i.e. the curvature of the emitting surface) and cosmological effects.

Details of the model are presented in [3] (see also Daigne et al., these proceedings).

CP1133, *Gamma Ray Bursts, 6th Huntsville Symposium*
edited by C. Meegan, N. Gehrels, and C. Kouveliotou

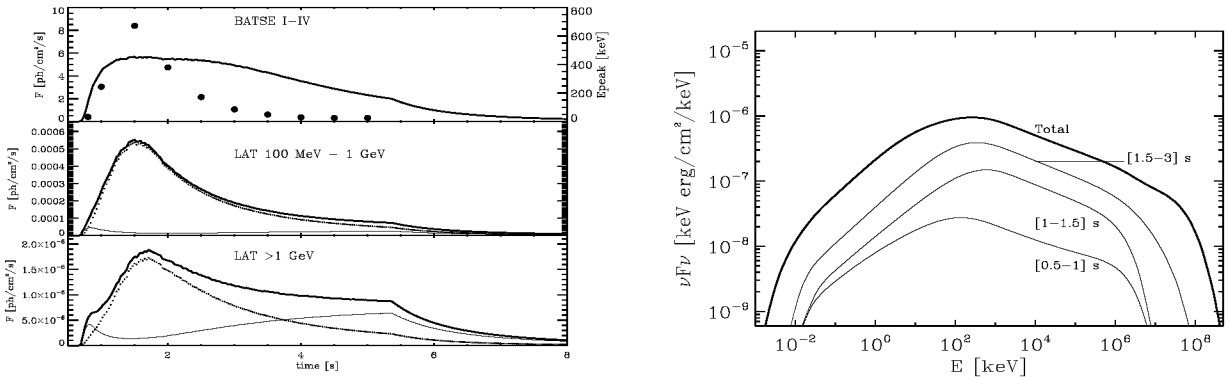

FIGURE 1. A single pulse burst in the "synchrotron case" with a high magnetic field. The injected kinetic power is $\dot{E} = 5 \times 10^{53}$ erg s^{-1}; the initial distribution of Lorentz factors is smoothly varying from Γ=100 in the front to Γ=400 in the rear part of the wind. The wind ejection lasted for t_w=2 s. The microphysics parameters are: $\varepsilon_B = \varepsilon_e = 1/3$; the relativistic electron distribution is described by $\zeta = 3 \times 10^{-3}$ and $p = 2.5$. *Left:* observed lightcurves in *BATSE* and *Fermi*-LAT energy range. The synchrotron (dotted line) and inverse Compton (thin line) components are shown. Filled circles show the time evolution of the peak energy in a given energy band. *Right:* observed time-integrated spectrum during the rise, the maximum, the early decay and the whole duration of the pulse.

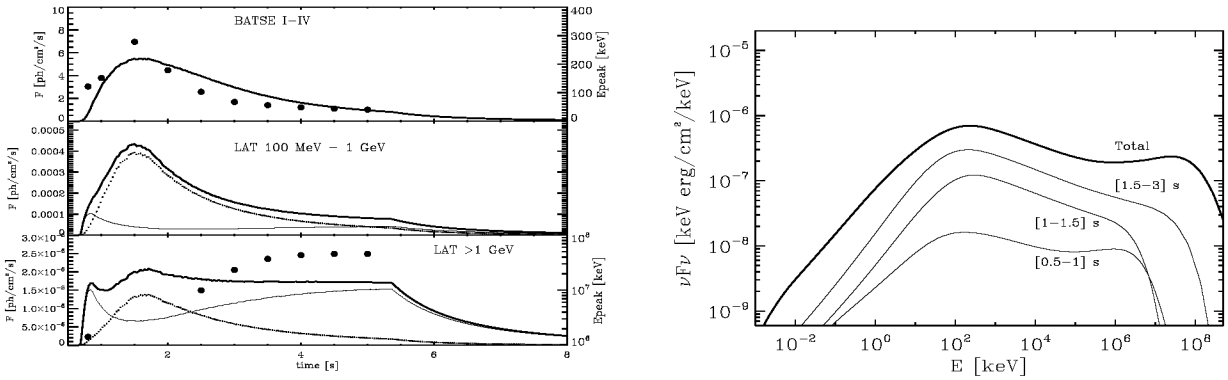

FIGURE 2. A single pulse burst in the "synchrotron case" with a low magnetic field. Same as in Fig. 1 except for the microphysics parameters: $\varepsilon_B = 5 \times 10^{-3}$, $\varepsilon_e = 1/3$, $\zeta = 2 \times 10^{-3}$ and $p = 2.5$. In this case the prominent spectral peak due to inverse Compton component occurrs also in the high energy band, as seen in the light curve corrseponding to *Fermi-LAT* energies.

EXAMPLES OF SYNTHETIC BURSTS: SPECTRAL EVOLUTION

We explored a broad region of the parameter space (parameters defining the dynamical evolution and microphysics parameters describing the conditions in the shocked region) and found two classes of broad-band spectra that can be expected: (i) 'synchrotron case' (Figs. 1, 2, 4) where the dominant process in the low energy (20 keV - 2 MeV) range is synchroton radiation; and (ii) 'inverse Compton case' (Fig. 3) where the synchrotron component peaks at lower energies and the dominant process in the (20 keV - 2 MeV) energy range is inverse Compton. The characteristics of GRB time profiles (e.g. [4] found that the pulse width decreases at higher energies and that the lower energy pulse lags the higher energy one) as well as the characteristic spectral parameters (e.g. [5], [6]) have been investigated in detail for low-energy bands, and thus our theoretical predictions can be verified by present observations. Our model predicts various behaviors in high-energy (GeV) bands, since the corresponding lightcurves are composed of two different components (synchrotron and inverse Compton) and their ratio evolves during a pulse; therefore the lightcurves and the spectral peak energy evolution differ in the low- and high-energy bands.

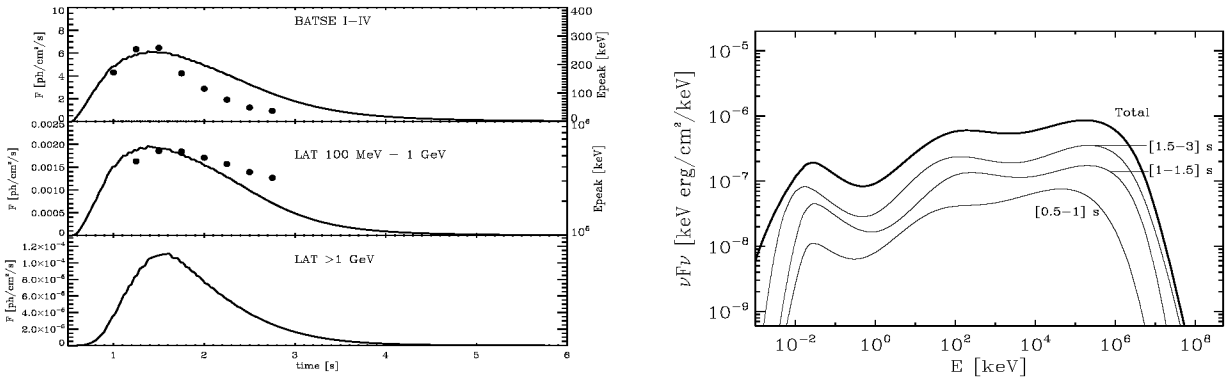

FIGURE 3. A single pulse burst in the "inverse Compton case". Same as in Fig.1 except that the initial distribution of the Lorentz factor varies from 100 to 600 and for the microphysics parameters we have: $\varepsilon_B = 10^{-2}$, $\varepsilon_e = 1/3$, $\zeta = 1$ and $p = 3.5$. In the left panel, the lightcurves observed both in the *BATSE+Fermi*-LAT energy range are entirely dominated by inverse Compton emission.

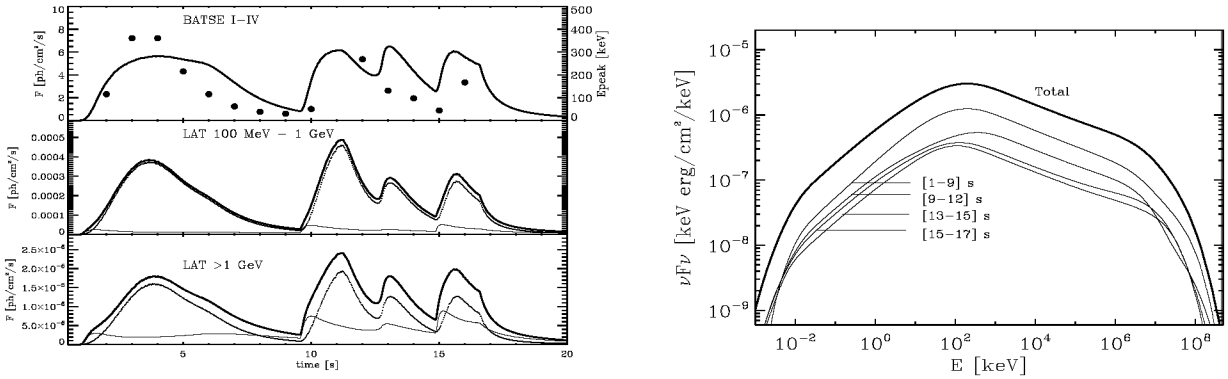

FIGURE 4. A multi-pulse burst in the "synchrotron case" with a high magnetic field. The dynamics is computed for the complex initial distribution of the Lorentz factor with Γ varying between 100 and 400, assuming a total duration of the relativistic ejection phase $t_w = 8$ s and an injected kinetic power $\dot{E} = 5 \times 10^{53}$ erg s^{-1}. The microphysics parameters are $\varepsilon_B = \varepsilon_e = 1/3$, $\zeta = 0.002$ and $p = 2.5$. The observed spectra integrated in time corresponding (approximately) to the durations of the respective pulses are shown.

CONCLUSIONS

We present the classes of synthetic gamma-ray bursts that can be expected for various internal shock parameters regions. The spectral evolution and the corresponding lightcurves differ greatly for the "synchrotron case" and "inverse Compton case"; the forthcoming observations of the high energy (GeV) emission can be used to discriminate between burst classes and related parameter regions. Our study emphasizes the importance of a detailed broad band spectral modelling in the interpretation of the future observations and in the physical diagnostics based on *Fermi* data.

REFERENCES

1. M. Rees, P. Mészáros, *ApJ* **430**, L93-L96 (1994)
2. F. Daigne, R. Mochkovitch, *MNRAS* **296**, 275-286 (1998)
3. Z. Bosnjak, F. Daigne and G. Dubus, astro-ph/0811.2956 (2008)
4. J. Norris et al., *ApJ* **459**, 393-412 (1996)
5. E. Liang, V. Kargatis, *Nature* **381**, 49-51 (1996)
6. R.D. Preece et al., *ApjSS* **126**, 19-36 (2000)